Available online at www.sciencedirect.com
ScienceDirect
Nuclear Physics B Proceedings Supplement 00 (2012) 1–6
Nuclear Physics B Proceedings Supplement

Measurements of Quarkonium Production Cross-Sections with the CMS Experiment

Yu Zheng for the CMS Collabration

Department of Physics, Purdue University, West Lafayette, IN, USA

Abstract

Using large data samples of dimuon events, CMS has performed detailed measurements of differential cross sections of J/Ψ, Ψ(2S) and ϒ(nS) states, as a function of transverse momentum in several rapidity bins. The measurements reach significantly higher transverse momentum than previously reported. The quarkonium production cross-sections are compared with recent predictions in the context of NLO nonrelativistic QCD.

In this talk, we will present a new measurement on ϒ(nS) production cross sections in proton-proton collisions at $\sqrt{s}$ = 7 TeV. We report the cross section results integrated over the transverse momentum range $p_{\mathrm{T}} < 50$ GeV/c and rapidity range $|y| < 2.4$. We also report the measurement of the ϒ(nS) differential cross sections as a function of transverse momentum and rapidity and the cross section ratios ϒ(2S)/ϒ(1S) and ϒ(3S)/ϒ(1S).

Finally, we report the very recent measurement of χ_{c2} / χ_{c1} production cross-sections, differentially in p_{T}, extending to p_{T} = 25 GeV/c, thereby providing an important test of QCD calculations at higher p_{T} than previously possible.

Keywords: quarkonium, charmonium, bottomonium, χ_c

1. Introduction

No existing theoretical approach successfully reproduces both the differential cross section and the polarization measurements of the J/Ψ or ϒ states [1]. Quarkonium production at hadron colliders provides important tests of calculations in the context of both perturbative and non-perturbative quantum chromodynamics (QCD), via measurements of production cross sections and polarizations. Studying quarkonium hadroproduction at higher center-of-mass energies and over a wider rapidity and momentum range will facilitate significant improvements in our understanding of the processes involved.

A detailed description of the CMS detector can be found in [2]. Its central feature is a superconducting solenoid of 6 m internal diameter, providing a magnetic field of 3.8 T. Within the field volume are the silicon pixel and strip tracker, the crystal electromagnetic calorimeter, and the brass/scintillator hadron calorimeter. Muons are measured in gas-ionisation detectors embedded in the steel return yoke. In addition to the barrel and endcap detectors, CMS has extensive forward calorimetry. The muons are measured in the pseudorapidity window $|\eta| < 2.4$, with detection planes made of three technologies: Drift Tubes, Cathode Strip Chambers, and Resistive Plate Chambers.

The paper is organized as follows. Section 2 presents the J/Ψ and Ψ(2S) prompt and non-prompt cross section results and comparisons to the theory predictions. In Sec. 3, the ϒ(nS) cross section results and comparisons to other experiments and to the theory predictions are presented. Finally, Section 4 presents a measurement of the χ_{c2}/χ_{c1} cross-section ratio.

2. Charmonia

CMS has recently published the measurement of the J/Ψ and Ψ(2S) meson production cross sections in pp

collisions at $\sqrt{s}$ =7 TeV. The data correspond to an integrated luminosity of 36.7 pb^{-1} [3].

Figure 1 shows the measured "inclusive" cross sections as a function of p_{T} for the various rapidity bins, compared with the ones published in [4], which are statistically independent and remain of interest since they cover a lower p_{T} range. A nice agreement is observed.

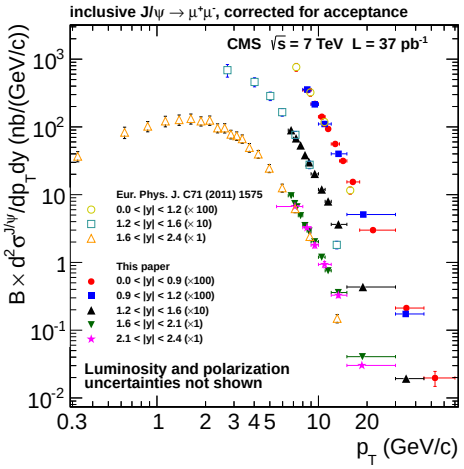

Figure 1: Measured differential cross section for J/Ψ inclusive production as a function of p_{T} for five rapidity bins, plotted with the results published in [4], which extend to a lower p_{T} range. (The multiplicative factors - showing as additive offsets in log scale - are used to achieve a convenient graphical separation of the measurements from different rapidity bins.)

To estimate the J/Ψ fraction from b-hadron decays, a two-dimensional fit is performed, in which the pdfs and fit procedure are the same as those described in Ref. [4]. The variables used for the two-dimensional fits are the dimuon invariant mass and the "pseudo proper decay length" $\ell_{J/\Psi}$, defined as the most probable value of the transverse distance between the dimuon vertex and the primary vertex, corrected by the transverse Lorentz boost of the J/Ψ. The measured b-fraction values for J/Ψ and Ψ(2S) mesons are shown in Fig. 2. The uncertainties shown are statistical and systematic, and the measured values are plotted as a function of p_{T}.

Prompt and non-prompt cross-sections have also been determined, as shown in Fig. 3 and Fig. 4. The nonrelativistic QCD (NRQCD) prediction includes indirect production in the J/Ψ case, so it can be directly compared to the data: good agreement is found in both the J/Ψ and the Ψ(2S) case. For non-prompt production an overall scale difference is found in the Ψ(2S) case, possibly due to the large uncertainty of $B \to \Psi(2S)$ decay rates: in general, for both states, the observed cross-sections spectrum seems to fall more rapidly than the Fixed Order plus Next-to-Leading Log-

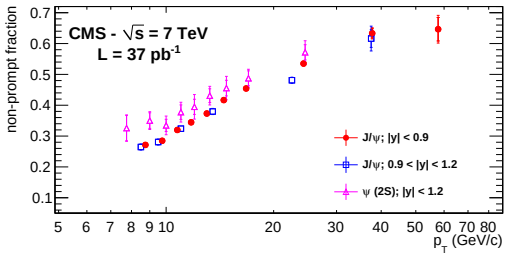

Figure 2: Fitted J/Ψ and Ψ(2S) non-prompt fractions plotted as a function of p_{T} for the rapidity region: $0 < |y| < 1.2$.

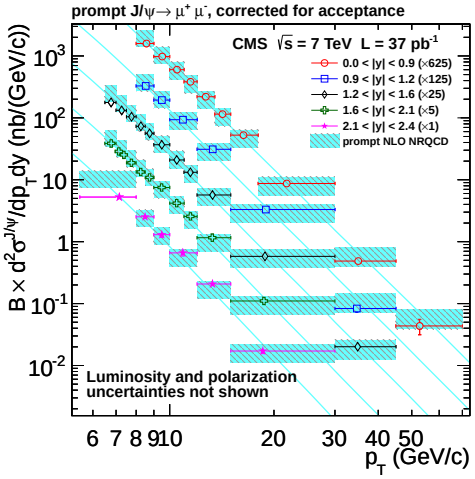

(a) J/Ψ

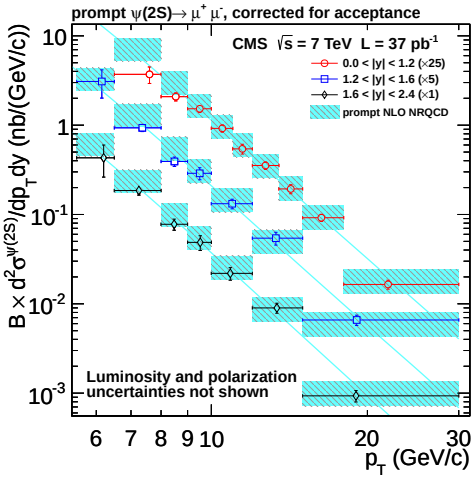

(b) $\Psi(2S)$

Figure 3: Measured differential cross section for prompt J/Ψ (a) and Ψ(2S) (b) production as a function of p_{T} for the different rapidity bins. The blue colored histograms indicate the theoretical predictions from NRQCD calculations, the lines are added only for illustrative purposes.

arithms (FONLL) prediction at high p_T. The resulting prompt and non-prompt $\Psi(2S)$ to J/Ψ cross section ratios are shown in Fig. 5 as a function of p_T.

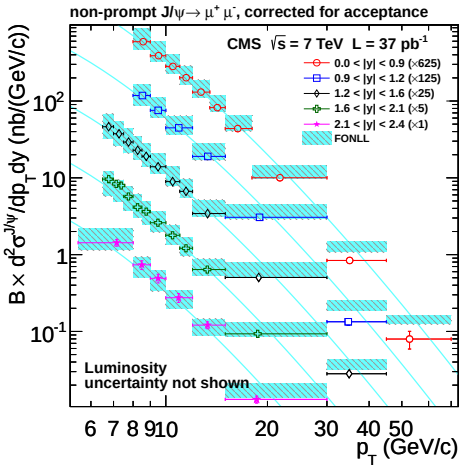

(a) J/Ψ

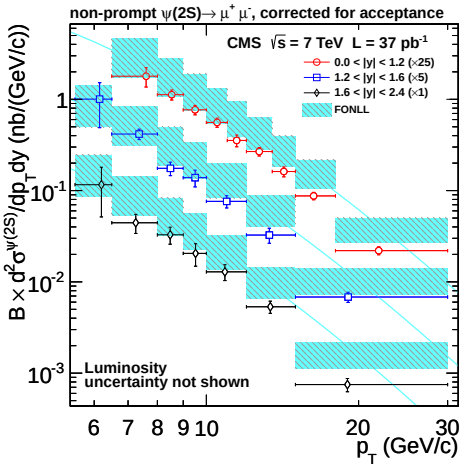

(b) $\Psi(2S)$

Figure 4: Measured differential cross section for non-prompt J/Ψ (a) and $\Psi(2S)$ (b) production as a function of p_T for the different rapidity bins. The blue colored histograms indicate the theoretical predictions from FONLL calculations, the lines are added only for illustrative purposes.

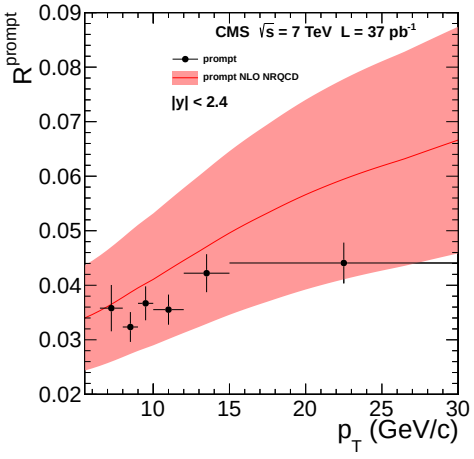

(a)

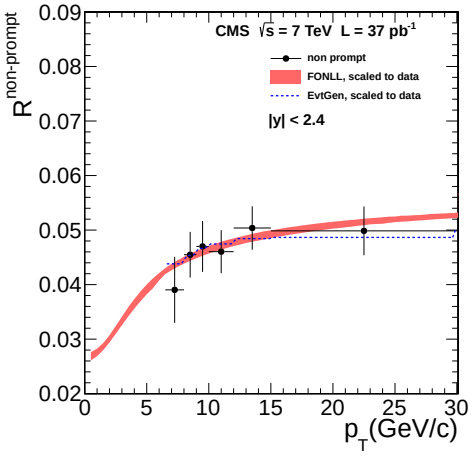

(b)

Figure 5: Measured value of the $\Psi(2S)$ to J/Ψ differential cross section ratio for prompt (a) and non-prompt (b) production, averaged over rapidity and plotted as a function of p_T. The top plot also includes the comparison with the NRQCD prediction, while the bottom plot shows the predictions of the theoretical models used to determine $\mathcal{B}(B \to \Psi(2S)X)$, after the theoretical curves have been rescaled to the measured value of the inclusive $\mathcal{B}(B \to \Psi(2S)X)$ branching fraction. The shaded bands show the uncertainties on the theoretical predictions. The error bars give the total uncertainties on the measurements; polarization uncertainties are not included.

3. Bottomonia

The measurements of the Υ(nS) differential production cross sections in the dimuon channel in proton-proton collisions at $\sqrt{s}$= 7 TeV [5, 6] with the CMS experiment are summarized in this section. The results have been presented in two ways, both in the form of acceptance-corrected cross sections and within the muon fiducial acceptance. The Υ(nS) p_T differential fiducial cross-section results for the rapidity region $|y^{\Upsilon}| < 2.4$ is shown in Fig. 6. The Υ(nS) p_T-integrated, rapidity-differential fiducial cross-section results compared to PYTHIA [7] are shown in Fig. 7. The ratios of Υ(nS) p_T-differential fiducial cross sections are shown in Fig. 8. The ratios increase with p_T^{Υ}. The Υ(3S) is expected not to have a significant feed-down component

unlike the Υ(2S) and Υ(1S), therefore a possible explanation for the $p_{\rm T}$ dependence of the ratios is that the $p_{\rm T}$ dependence of the cross section for direct production of each Υ resonance is the same, and the softening of the spectrum is due to feed-down from higher mass states.

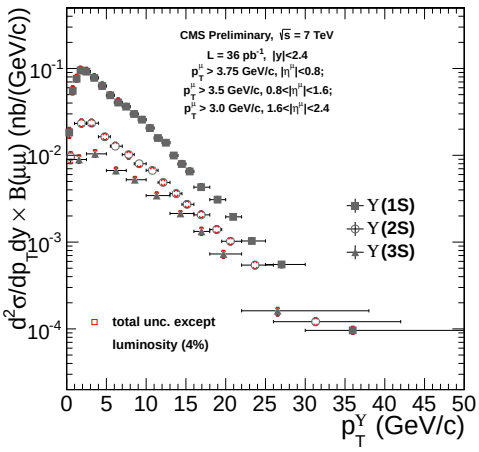

Figure 6: Differential fiducial cross sections of the Υ(nS) as a function of $p_{\rm T}^{\Upsilon}$ in the rapidity range $|y| < 2.4$.

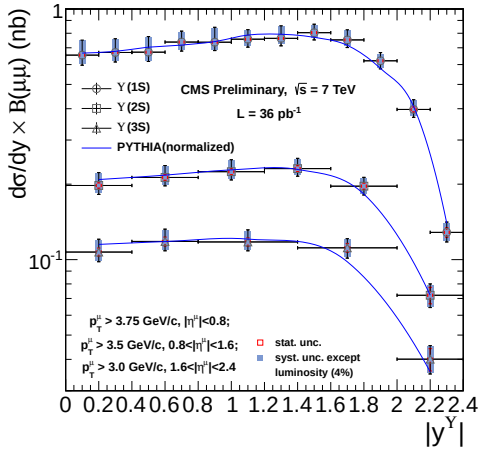

Figure 7: Differential fiducial cross sections of the Υ(nS) as a function of rapidity, compared to PYTHIA predictions.

The Υ(1S) $p_{\rm T}$ differential cross-section results compared with various theoretical models are shown in Fig. 9. Each of the predictions is for unpolarized Υ(nS) production, and both the measurement and the prediction are for $|y^{\Upsilon}| < 2.0$. The comparison is made to the CASCADE MC generator in the FONLL framework [8] including feed-down from $\chi_{b(1P)}$ and $\chi_{b(2P)}$, PYTHIA, the Color Evaporation Model (CEM) [9] (no

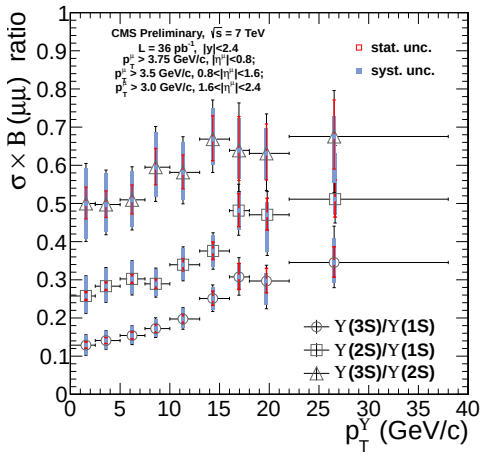

Figure 8: Ratios of differential fiducial cross sections of the Υ(nS) as a function of $p_{\rm T}^{\Upsilon}$ in the rapidity range $|y^{\Upsilon}| < 2.4$.

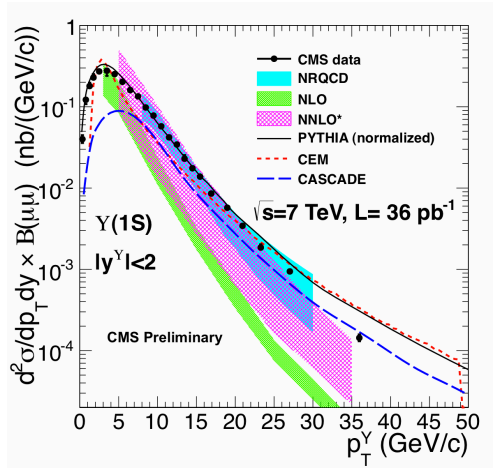

Figure 9: Differential cross section of the Υ(1S) as a function of $p_{\rm T}^{\Upsilon}$ in the rapidity range $|y^{\Upsilon}| < 2$, and comparison to various theoretical predictions. The width of a band indicates an estimate of the uncertainty in the prediction by the author of the prediction.

feed-down estimation is available), NRQCD to next-to-leading order (NLO) including feed-down as described in Ref. [10], the Color Singlet Model (CSM) to NLO and to next-to-next-to-leading order (NNLO*) [11] where the feed-down is accounted for by scaling the Υ(1S) direct production cross section by a factor 2 for the inclusive Υ(1S) cross section. The theory predictions are private communications [12, 13, 14, 15] as no predictions for unpolarized Υ(nS) production are available in the literature at $\sqrt{s}$= 7 TeV. Our measured Υ(1S) cross section is lower than the CEM prediction at low p_T Υ. The data agree well with NRQCD above $p_{\rm T}$ =10 GeV/c for Υ(1S). The NLO CSM cannot describe

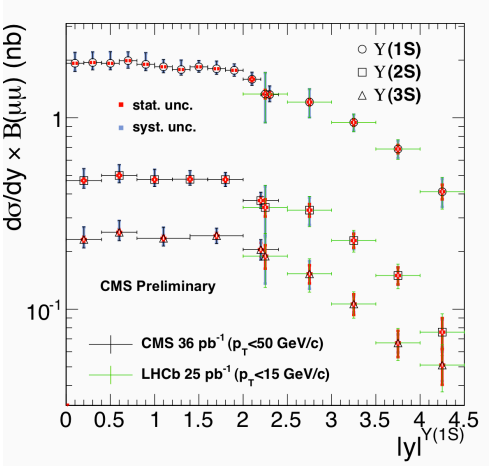

Figure 10: Differential production cross sections of the Υ(nS) as a function of rapidity and comparison to LHCb results.

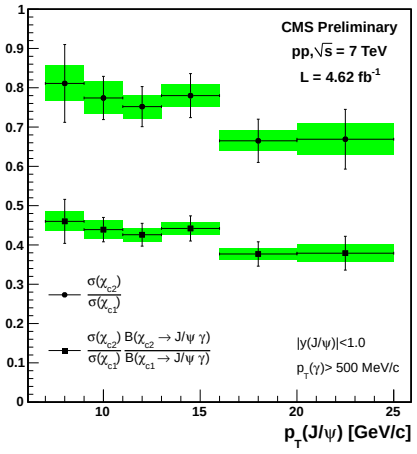

Figure 11: χ_{c2}/χ_{c1} cross section ratio (circles) and ratio of the cross section multiplied by the branching ratios to J/Ψ+γ (squares). The green band corresponds to the systematic error and the error bars to the statistical error. For the ratio of cross sections the 10% error derived from the branching fractions is not shown.

the data while the NNLO* CSM shows better agreement with data within the large uncertainties. The Υ(nS) rapidity-differential cross sections measured with CMS and the LHCb results [16] are shown in Fig. 10. The results are complementary in their rapidity coverage and consistent within the uncertainties in the region of overlap.

4. χ_c States

A measurement of the relative prompt production rate of χ_{c2} and χ_{c1}, with 4.62 fb^{-1} of data collected at LHC at $\sqrt{s}$= 7 TeV is presented [17]. The measurement is based on the reconstruction of the radiative decays to J/Ψ plus photon, with the low transverse momentum photons (in the GeV range) being detected through their conversion in electron-positron pairs. The photon selection is implemented as follows. Photon conversions are characterized by an electron-positron pair originating from a common vertex. The e^+e^- invariant mass is consistent with zero and the two tracks are parallel at the conversion vertex and open only in the transverse plane because of the magnetic field generated by the CMS solenoid. Any conversion building a pair whose invariant mass falls in the range between 0.11 and 0.15 GeV/c^2, corresponding to a 2σ window around the reconstructed π^0 mass, is rejected. In order to restrict the measurement to the prompt signal component, the pseudo-proper decay length of the J/Ψ, defined in [4], is required to be less than 30 mm.

The results of the measurement of $\frac{\sigma(pp\to\chi_{c2}+X)}{\sigma(pp\to\chi_{c1}+X)} \times \frac{BR(\chi_{c2}\to J/\Psi\gamma)}{BR(\chi_{c1}\to J/\Psi\gamma)}$ and $\frac{\sigma(pp\to\chi_{c2}+X)}{\sigma(pp\to\chi_{c1}+X)}$ for the kinematic range

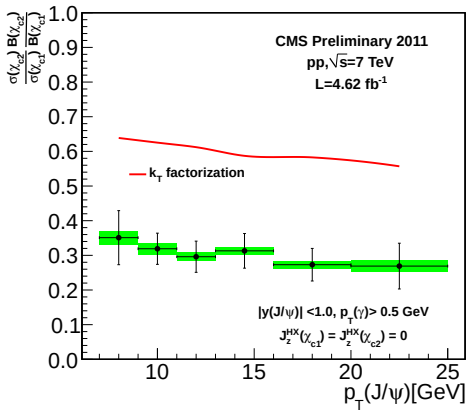

Figure 12: Comparison of the measured ratio of cross sections multiplied by the branching ratios with predictions from the k_t-factorization.

$p_T(\gamma) > 0.5$ GeV/c and $|y^{J/\Psi}| < 1.0$ are shown in Fig. 11. The results are compared to k_t-factorization and NLO NRQCD theoretical approaches as shown in Fig. 12 and Fig. 13. As the k_t-factorization model predicts that both χ_{c1} and χ_{c2} are produced with helicity zero in the helicity frame, for a proper comparison the ratio was recalculated under this assumption. The k_t-factorization cannot describe the measurement. The NLO NRQCD predictions were produced without a cut on the photon

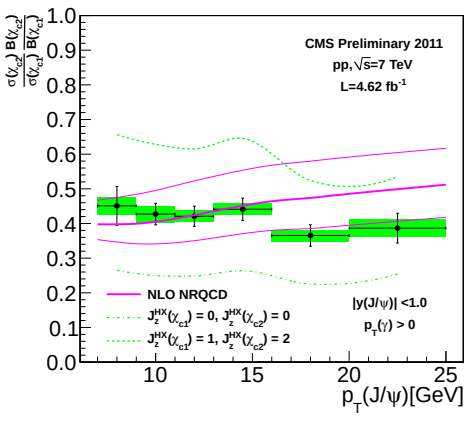

Figure 13: Comparison of the measured ratio of cross sections multiplied by the branching ratios with predictions from NLO NRQCD.

transverse momentum. A correction factor derived from Monte Carlo is applied to extrapolate the measurements down to zero photon p_{T}.

5. Summary

In summary, CMS has measured the J/Ψ, Ψ(2S) and ϒ(nS) meson production cross sections in pp collisions at $\sqrt{s}$ = 7 TeV. The J/Ψ and Ψ(2S) cross sections and their ratio have been measured as a function of the meson transverse momentum p_{T} (up to 70 GeV/c for the J/Ψ and to 30 GeV/c for the Ψ(2S)) in several rapidity ranges assuming null polarization in the prompt production. Results have been compared to NRQCD and FONLL predictions respectively, finding a reasonable agreement except for non-prompt cross-sections at high p_T. The inclusive branching fraction $\mathcal{B}(B \to \Psi(2S)X)$ is extracted from the ratio of the non-prompt cross sections, improving the relative uncertainty on the previous world average by a factor of three. The differential cross sections for each ϒ(nS) state and the cross-section ratios have been measured as a function of p_T^{Υ} and rapidity and compared to various theory predictions. The relative prompt production rate of χ_{c2} and χ_{c1} is measured. The result is among the most accurate and precise measurements of χ_c production in hadron collisions, and extends the explored p_T range of previous works. Possible systematic uncertainties coming from the unknown polarization of the χ_c are also investigated.

References

[1] N. Brambilla et al., Heavy quarkonium: progress, puzzles, and opportunities, The European Physical Journal C - Particles and Fields 71 (2011) 1–178, 10.1140/epjc/s10052-010-1534-9. URL http://dx.doi.org/10.1140/epjc/s10052-010-1534-9

[2] The CMS Collaboration, The CMS experiment at the CERN LHC, Journal of Instrumentation 3 (08) (2008) S08004. URL http://stacks.iop.org/1748-0221/3/i=08/a=S08004

[3] The CMS Collabration, J/Ψ and Ψ(2S) production in pp collisions at $\sqrt{s}$ = 7TeV, Journal of High Energy Physics 2012 (2012) 1–46, 10.1007/JHEP02(2012)011. URL http://dx.doi.org/10.1007/JHEP02(2012)011

[4] The CMS Collaboration, Prompt and non-prompt J/Ψ production in pp collisions at $\sqrt{s}$ = 7TeV, The European Physical Journal C - Particles and Fields 71 (2011) 1–26, 10.1140/epjc/s10052-011-1575-8. URL http://dx.doi.org/10.1140/epjc/s10052-011-1575-8

[5] The CMS Collabration, Upsilon production cross section in pp collisions at $\sqrt{s}$ = 7 TeV, Phys. Rev. D 83 (2011) 112004. doi:10.1103/PhysRevD.83.112004. URL http://link.aps.org/doi/10.1103/PhysRevD.83.112004

[6] The CMS Collabration, Measurement of the Upsilon(nS) production cross section in pp collisions at $\sqrt{s}$ = 7 TeV, BPH-11-001.

[7] V. M.Bargiotti, Heavy Quarkonia sector in PYTHIA 6.324 : tuning, validation and perspectives at LHC(b), Report No. LHCb-2007-042. URL http://cdsweb.cern.ch/record/1042611.

[8] H. Jung, et al., The CCFM Monte Carlo generator CASCADE 2.2.0arXiv:1008.0152, doi:10.1140/epjc/s10052-010-1507-z.

[9] A. D. Frawley, T. Ullrich, R. Vogt, Heavy flavor in heavy-ion collisions at RHIC and RHIC II, Phys. Rept. 462 (2008) 125. arXiv:0806.1013, doi:10.1016/j.physrep.2008.04.002.

[10] K. Wang, Y.-Q. Ma, K.-T. Chao, ϒ(1S) prompt production at the Tevatron and LHC in nonrelativistic QCD, Phys. Rev. D 85 (2012) 114003. doi:10.1103/PhysRevD.85.114003. URL http://link.aps.org/doi/10.1103/PhysRevD.85.114003

[11] J.-P. Lansberg, J/ψ production at $\sqrt{s}$ = 1.96 and 7 TeV: Color-Singlet Model, NNLO* and polarisationarXiv:1107.0292.

[12] K.-T. Chao private communication.

[13] J.-P. Lansberg private communication.

[14] H. Jung private communication.

[15] R. Vogt private communication.

[16] The LHCb Collabration, Measurement of Upsilon production in pp collisions at $\sqrt{s}$ = 7 TeVarXiv:1202.6579.

[17] The CMS Collabration, Measurement of $\sigma(\chi_{c2})/\sigma(\chi_{c1})$ at $\sqrt{s}$ = 7 TeV, CMS-PAS-BPH-11-010.

[18] G. T. Bodwin, E. Braaten, G. P. Lepage, Rigorous QCD analysis of inclusive annihilation and production of heavy quarkonium, Phys. Rev. D51 (1995) 1125. doi:10.1103/PhysRevD.51.1125.

[19] P. Cho, A. K. Leibovich, Color-octet quarkonia production, Phys. Rev. D53 (1996) 150. doi:10.1103/PhysRevD.53.150.

[20] P. Cho, A. K. Leibovich, Color-octet quarkonia production II, Phys. Rev. D53 (1996) 6203. doi:10.1103/PhysRevD.53.620.